Self-trapping of scalar and vector dipole solitary waves in Kerr media

Wei-Ping Zhong, Milivoj R. Belić, Gaetano Assanto, Boris A. Malomed, and Tingwen Huang

Self-trapping of scalar and vector dipole solitary waves in Kerr media

Wei-Ping Zhong[1], Milivoj R. Belić[2,3], Gaetano Assanto[4], Boris A Malomed[5], and Tingwen Huang[2]

[1]*Department of Electronic and Information Engineering, Shunde Polytechnic, Guangdong Province, Shunde 528300, China*

[2]*Texas A & M University at Qatar, 23874 Doha, Qatar*

[3]*Institute of Physics, University of Belgrade, P. O. Box 57, 11001 Belgrade, Serbia*

[4]*NooEL, Nonlinear Optics and OptoElectronics Lab, University of Rome "Roma Tre", 00146 Rome, Italy*

[5]*Department of Physical Electronics, School of Electrical Engineering, Faculty of Engineering, Tel Aviv University, Tel Aviv 69978, Israel*

Abstract: We report solutions for expanding dipole-type optical solitary waves in 2D Kerr media with the self-focusing nonlinearity, using exact analytical (Hirota) and numerical methods. Such localized beams carry intrinsic vorticity and exhibit symmetric shapes for both scalar and vector solitary modes. When vector beams are close to the scalar limit, simulations demonstrate their stability over propagation distances exceeding 50 diffraction lengths. In fact, the continuous expansion helps the vortical beams to avoid the instability against the splitting, collapse or decay, making them "convectively stable" patterns.

PACS number: 42.81.Dp, 42.65.Sf.

1. Introduction

Spatial solitons are stable self-trapped beams propagating in nonlinear media, for which diffraction is exactly balanced by self-focusing [1]. In particular, vector solitons consist of different components with comparable intensities, which all contribute to the induced increase of the refractive index in the material. In optics, spatial vector solitons can be formed by either copropagating or counterpropagating interacting beams [2]. In the basic form, they are represented by shape-preserving self-localized solutions of coupled nonlinear evolution partial differential equations (PDEs) [3]. Spatial vector solitons in the form of two-color self-trapped copropagating beams were discussed in nonlocal Kerr media [4, 5] and experimentally observed in nematic liquid crystals by Alberucci *et al*. [6]. Vector solitons with counterpropagating beams were reported by Izdebskaya *et al*. [7]. In the general case, several beams can combine to produce multi-component vector solitons. Another variety of stable two-color solitary beams is supported by the three-wave mixing in quadratically nonlinear ($\chi^{(2)}$) media [8]. One- and two-dimensional (1D and 2D) spatial $\chi^{(2)}$ solitons (alias "simultons") were created experimentally [9] and studied in detail theoretically, see e.g. reviews [10]. Their spatiotemporal counterparts have been investigated as well [11].

The existence of dipole-mode vector solitons (or "dipoles", for simplicity) was predicted theoretically [12, 13] and verified experimentally [14]. This kind of optical solitons originates from the trapping of a dipole HG_{01}-type mode in the waveguide induced by a copropagating fundamental spatial soliton. It was shown that, while several other topologically arranged structures may be created in this setting, only the dipole solitary mode is expected to give rise to a family of dynamically robust vector solitons [15, 16]. Stationary 2D dipole-mode solitons were observed in optical media with thermal nonlinearity [17]. It was shown that the stability of dipole solitons in nonlocal nonlinear waveguides crucially depends on the waveguide shape [18], and that elliptically shaped dipole solitons are expected in media with an anisotropic quasi-local nonlinearity [19]. In all of the aforementioned studies, solitons were obtained either numerically or by means of variational or other approximations. However, no exact solutions were found for dipole vector solitons to date.

In this paper, we report the first (to the best of our knowledge) *exact* 2D analytical solutions for dipole-mode scalar and vector solitary waves in local Kerr medium. Such solutions, constructed using the separation of variables and the Hirota bilinear method, are nonstationary and gradually expanding in propagation, similarly to necklace-shaped soliton

patterns [20]. It is well known that stationary solitons in 2D Kerr media are always unstable against collapse or decay, due to the critical character of the local cubic self-attractive nonlinearity in the 2D setting. Moreover, 2D ring-shaped solitons with embedded vorticity are subject to a still stronger instability against splitting of the ring under the action of azimuthal perturbations [21, 22]. Nonetheless, we demonstrate hereby that a part of the expanding solitary waves (those close enough to the scalar limit) remain stable over a long evolution. In fact, the continuing expansion helps avoiding splitting, collapse, or decay. In that sense, they may be called *convectively stable* patterns, following the analogy with the commonly known concept of convective instability. An analytical explanation of this effective stability is given below, alongside the numerical simulations.

The paper is organized as follows. In Sec. 2 we describe the model governing the dynamics of dipole beams with two mutually incoherent components copropagating in a local Kerr medium. We discuss the lowest-order dipole solitary waves with two components in Sec. 3, where we study their properties numerically. We address the stability of dipole vector beams in Sec. 4, and draw conclusions in Sec. 5.

2. The model and the solution method

To model the dynamics of scalar and vector beams consisting of N mutually incoherent components copropagating in a Kerr medium, we use coupled (2+1)D nonlinear Schrödinger equations for the slowly varying envelopes $u_n(z, r, \varphi)$ ($n = 1, 2, \cdots, N$), where r and φ are the polar coordinates in the transverse plane. The dimensionless form of the equations is [23]

$$i\frac{\partial u_n}{\partial z} + \frac{1}{2}\nabla_\perp^2 u_n + f(I)u_n = 0, \tag{1}$$

where the propagation distance, z, and the transverse Cartesian coordinates, x and y, are measured in units of $(L_D / k)^{1/2}$ and the diffraction length L_D, respectively (k is the carrier's wavenumber). The nonlinearity $f(I)$ is proportional to the total intensity of the beam, $f(I) = I = \sum_{n=1}^{N} |u_n|^2$. Hence Eq. (1) may be considered as a 2D version of the Manakov's system, and the paraxial diffraction is accounted for by the transverse Laplacian $\nabla_\perp^2 = \frac{\partial^2}{\partial r^2} + \frac{1}{r}\frac{\partial}{\partial r} + \frac{1}{r^2}\frac{\partial^2}{\partial \varphi^2}$, written in polar coordinates.

To find solutions to Eq. (1), we look for the optical field in the form of

$$u_n(r, \varphi, z) = V(z, r)\phi_n(\varphi), \tag{2}$$

with the self-consistency condition $\sum_{n=1}^{N} |\phi_n(\varphi)|^2 = 1$. Then, substituting Eq. (2) into Eq. (1), the separation of variables leads to the following two equations:

$$-\frac{1}{\phi_n}\frac{d^2\phi_n}{d\varphi^2} = m^2, \tag{3a}$$

$$\frac{2r^2}{V}\left[i\frac{dV}{dz} + \frac{1}{2}\left(\frac{\partial^2 V}{\partial r^2} + \frac{1}{r}\frac{\partial V}{\partial r}\right) + |V|^2 V\right] = m^2, \tag{3b}$$

where $m \geq 0$ is an integer, see Refs. [24, 25]. Obvious solutions to Eq. (3a) are $\phi_n(\varphi) = A_n \cos(m\varphi) + B_n \sin(m\varphi)$, (hence, m may be considered as a topological charge), with complex coefficients A_n and B_n obeying conditions

$\sum_{n=1}^{N} \mathrm{Re}\left(A_n B_n^*\right) = 0$ and $\sum_{n=1}^{N} |A_n|^2 = \sum_{n=1}^{N} |B_n|^2 = 1$. In this paper, we focus on the two-component $(N = 2)$ case and

choose the corresponding coefficients as follows:

$$A_1 = 1, \qquad B_1 = iq, \qquad (4a)$$

$$A_2 = 0, \qquad B_2 = \sqrt{1 - q^2}, \qquad (4b)$$

where parameter $q \in [0,1]$ determines the modulation depth of the beam. In the limit of $q = 0$, Eqs. (4) represent the incoherent superposition of two modes, whereas for $q = 1$ they correspond to the scalar solitary wave. For a dipole solitary mode with topological charge $m = 1$, Eq. (3b) can be written as:

$$i \frac{\partial V}{\partial z} + \frac{1}{2}\left(\frac{\partial^2 V}{\partial r^2} + \frac{1}{r}\frac{\partial V}{\partial r} - \frac{V}{r^2}\right) + |V|^2 V = 0, \qquad (5)$$

Next, we aim at obtaining some analytical solutions to Eq. (5), represented in the Hirota bilinear form. To this end, we make use of the following transformation: $V = r\dfrac{g(r,z)}{f(r,z)}$, where $g(r,z)$ is a complex function and $f(r,z)$ is a real one. Substituting these into Eq. (5) we obtain the bilinear forms as:

$$H_1[g \cdot f] = 0, \qquad (6a)$$

$$H_2[f \cdot f] = 2r^2 g g^*, \qquad (6b)$$

with $H_1 = irD_z + \frac{1}{2}rD_r^2 + \frac{3}{2}D_r$, $H_2 = D_r^2$, where the star indicates for the complex conjugation. Furthermore D_r

is Hirota's bilinear derivative operator [26, 27], defined as $D_r[g(r) \cdot f(r)] = \left(\dfrac{\partial}{\partial r} - \dfrac{\partial}{\partial r'}\right)g(r)f(r')\Big|_{r=r'}$. To find soliton

solutions, we expand functions $g(r,z)$ and $f(r,z)$ as power series of a parameter ε:

$$g(r,z) = \varepsilon g_1(r,z) + \varepsilon^3 g_3(r,z) + \cdots + \varepsilon^{2j+1} g_{2j+1}(r,z) + \cdots, \qquad f(r,z) = 1 + \varepsilon^2 f_2(r,z) + \varepsilon^4 f_4(r,z) + \cdots \varepsilon^{2j} f_{2j}(r,z) + \cdots.$$

Substituting $g(r,z)$ and $f(r,z)$ into the bilinear equations (6) and collecting terms pertaining to the same powers of ε, we obtain the following system of linear PDEs:

$$\varepsilon^1: \qquad H_1[g_1 \cdot 1] = 0, \qquad (7a)$$

$$\varepsilon^2: \qquad H_2[1 \cdot f_2 + f_2 \cdot 1] = 2r^2 g_1 g_1^*, \qquad (7b)$$

$$\varepsilon^3: \qquad H_1[g_1 \cdot f_2 + g_3 \cdot 1] = 0, \qquad (7c)$$

$$\varepsilon^4: \qquad H_2[g_1 \cdot f_2 + g_3 \cdot 1] = 2r^2\left(g_1 g_3^* + g_3 g_1^*\right). \qquad (7d)$$

....

Now, in order to get the first-order nonstationary soliton solution, we assume that $g(r,z)$ is truncated to $g_1(r,z)$, and $f(r,z)$ truncated to $f_2(r,z)$, i.e., $g_j(r,z) = 0$ for $j = 3,5,\cdots$ and $f_k(r,z) = 0$ for $k = 4,6,\cdots$. Thus,

we find that $f_2 = \dfrac{e^{D+D^*}}{4} \left[\dfrac{2(CC^* + 4z^2)}{C+C^*} \exp\left(-\dfrac{C+C^*}{CC^*+4z^2} r^2 \right) - r\sqrt{\pi} \left(\dfrac{CC^*+4z^2}{C+C^*} \right)^{3/2} erfi\left(r\sqrt{-\dfrac{C+C^*}{CC^*+4z^2}} \right) \right]$, and

$g_1 = \dfrac{1}{(C+2iz)^2} \exp\left[D - \dfrac{r^2}{C+2iz} \right]$, where $erfi(r)$ is the imaginary error function $erfi(ir)/i$, C and D are complex constants such that $C+C^* \neq 0$. Next, we set $\varepsilon = 1$ and obtain the first-order soliton solution of Eq. (5):

$$V^{(1)}(r,z) = \frac{r}{2(C+2iz)^2} \operatorname{sech}(\Omega + \Omega^* + \Omega_0) e^{\Omega - \Omega^* - i\Omega_0}. \tag{8}$$

where $\Omega = 2D - \dfrac{2r^2}{C+2iz}$ and $\Omega_0 = -4\ln\left|2(C+C^*)\right|$. Note that the argument of sech in Eq. (8) is automatically real.

In a similar fashion, we obtain the second and the Lth-order [28] nonstationary soliton solutions of Eq. (5) (see Appendix). Finally, making use of Eqs. (2) and (8), we arrive at the exact first-order solution of Eq. (1) for the dipole solitary mode:

$$u_n^{(1)}(r,\varphi,z) = \frac{r(A_n \cos\varphi + B_n \sin\varphi)}{2(C+2iz)^2} \operatorname{sech}(\Omega + \Omega^* + \Omega_0) e^{\Omega - \Omega^* - i\Omega_0}. \tag{9}$$

It is straightforward to see that $|u_n|$ vanishes at $r \to \infty$, i.e., Eq. (9) represents a localized, although nonstationary, bright solitary wave solution. Indeed, the radius of the ring structure corresponding to Eqs. (8) and (9) expands as $R \sim z$, while its squared amplitude decays as

$$\left(|A|^2\right)_{max} \sim z^{-2}. \tag{10}$$

3. Discussion

In this section we display and discuss solutions given in Eq. (9) for scalar and vector dipole modes. In most cases, we fix constants C and D, namely, $D = 0$ and $C = 2$ for the first-order solitary mode, and $D_1 = D_2 = 0$, $C_1 = 2$, $C_2 = 4$ for the second-order one.

For $q = 1$ in Eqs. (4), we obtain a scalar ring-shaped beam for $m = 1$. A typical example of such a vortex ring is shown in Fig. 1, along with the axisymmetric radial intensity distribution of solitary waves of various orders. The intensity is zero at the center, as it should be for vortex patterns. In the course of the evolution, this nonstationary vortex ring expands and gets attenuated in the radial direction. The number of layers (white annuli in the figure) in this scalar solitary wave is determined by its order L. The scalar soliton is represented as an incoherent superposition of two dipole solitary modes with $m = 1$ and $q = 1$. Accordingly, the dipole components can be written as $u_2 = 0$ and $u = u_1 = Ve^{i\varphi}$; hence u actually displays a simple isotropic vortex shape.
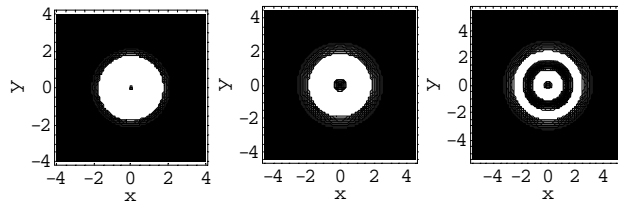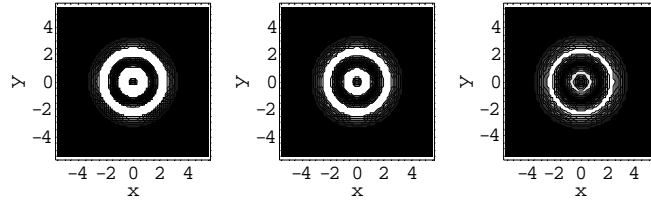
Fig. 1. Intensity distributions (nonzero in white annuli, zero in black areas) of the axially symmetric scalar mode, at $z = 0, 30, 50$, from left to right. Top and bottom rows display first- and second-order solitary modes, as given by Eq. (9).

Moreover, Fig. 2 displays a set of nonstationary radial intensity profiles, obtained from Eq. (8) for solitary waves of first and second orders. Increasing z, the intensity remains zero in $r = 0$ and $r = \infty$ (as it should be for vortical solitons, even nonstationary ones), while the structure expands in the radial direction and its peak gradually decays, in accordance with Eq. (10).
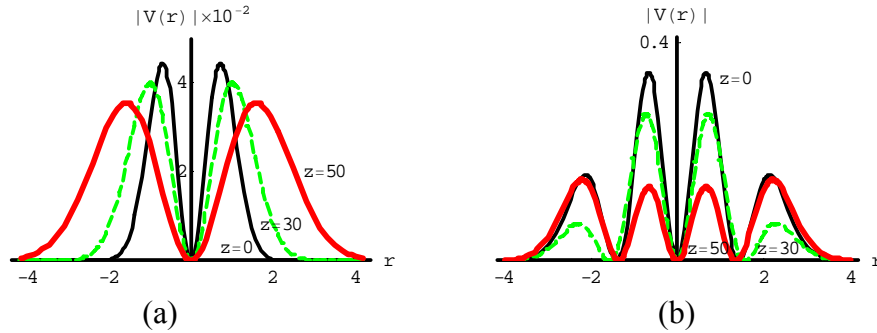

FIG. 2 (Color online) Nonstationary radial intensity distributions $\left|V(r)\right|$ at several values of the propagation distance, $z = 0, 30, 50$, as found from Eq. (8). Panels (a) and (b) display the first- and the second-order solitary-wave solutions.

Self-trapped localized structures with a large number of azimuthal lobes ("petals") may exhibit a strong effective stabilization even in self-focusing Kerr media [29, 30]. Fig. 3 and Fig. 4 display the propagation dynamics of the first- and second-order dipole vector modes, which exhibit similar patterns. These examples are obtained for $q = 0$ in Eqs. (4). In these solitary modes, the dipole structure is formed due to the interaction between the two components. Note that the intensity remains equal to zero at the center, as the solitary waves carry the intrinsic vorticity. As for scalar solitons, the structure expands in the radial direction. Note that the second-order dipole vector solitary waves form two layers, with the inner one more strongly modulated than its outer counterpart. As visible in Fig. 4, during evolution the peak intensity of the outer layer *increases* as compared with the inner one.
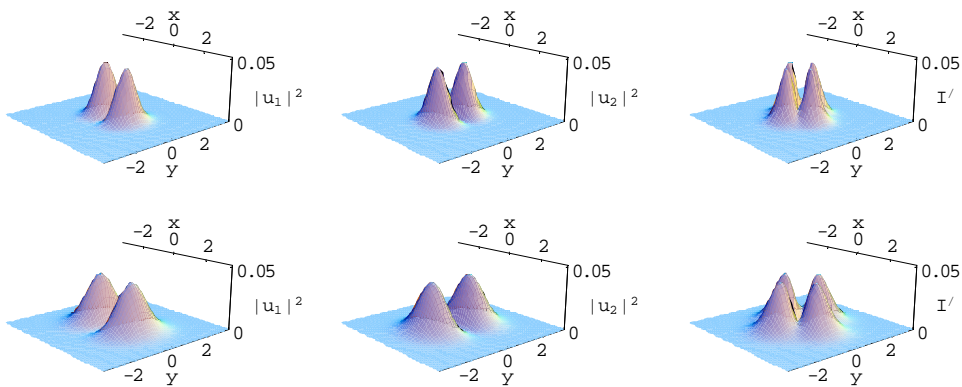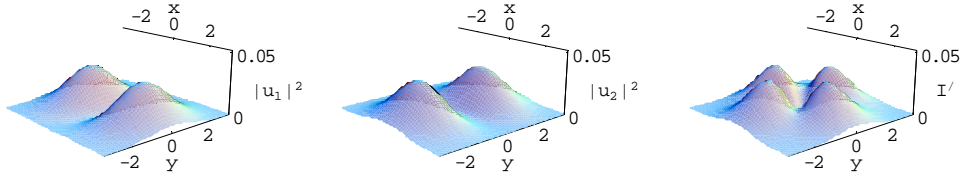
FIG. 3 (Color online) Evolution of the first-order dipole vector solitary waves with $q = 0$, shown for $z = 0, 30, 50$ from top to bottom. The total intensity of the solitary waves (the third column) is $I' = |u_1|^2 + |u_2|^2$.

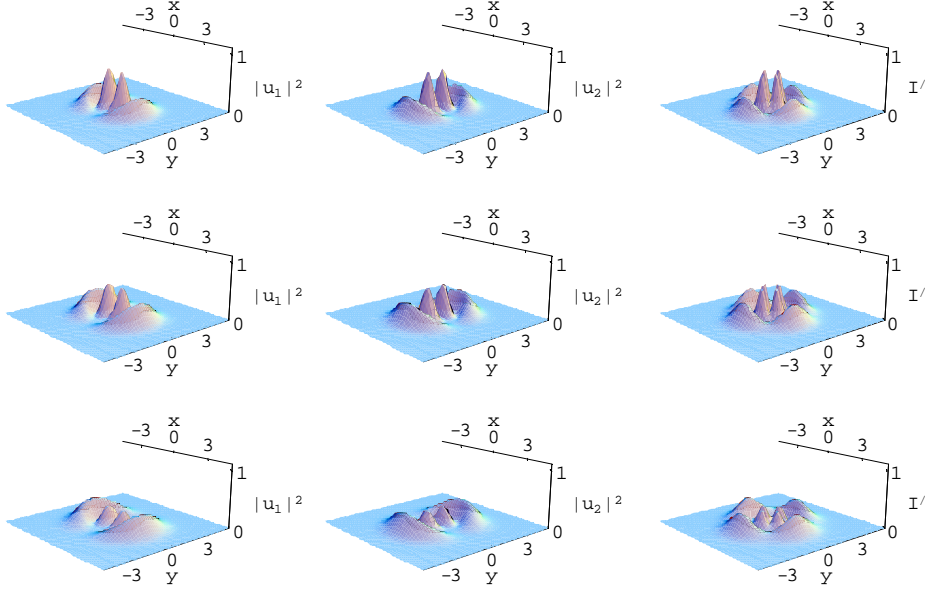

FIG. 4 (Color online) Same as Fig. 3, but for the second-order dipole vector solitary waves with $q = 0$.

The shape of the dipole vector modes is different for $q \to 1$ in Eqs. (4). With the increase in q, the components of the dipole vector solitary wave change their structure from the spiky pattern to the modulated vortex ring. The same trend can also be observed as $q \to 1$ in higher-order solitary modes. An example of the third-order dipole vector solitary wave in displayed in Fig. 5 for $q = 0.8$, $D_1 = D_2 = D_3 = 0$, and $C_1 = C_3 = 2$, $C_2 = 4$.
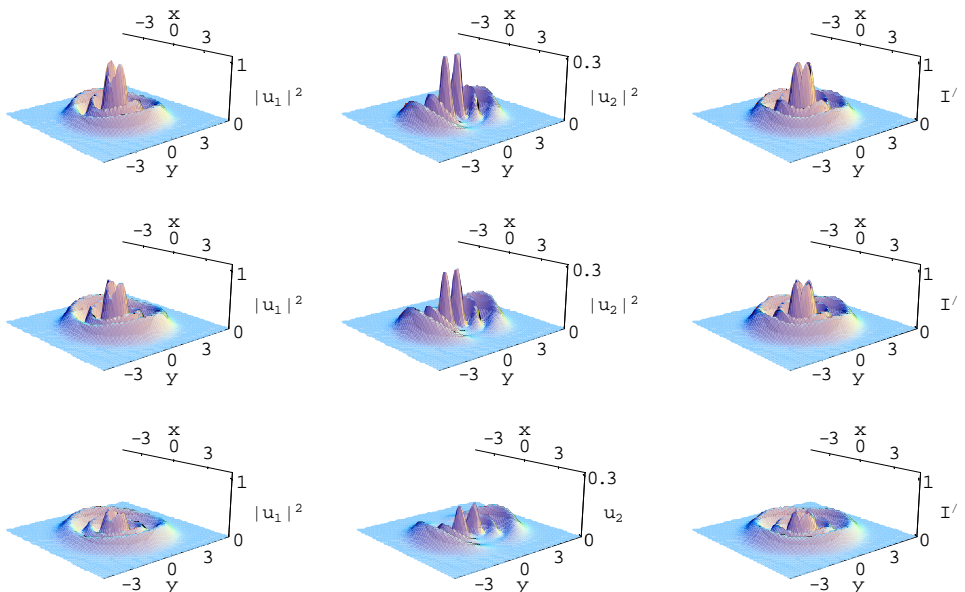
FIG. 5 (Color online) Same as Fig. 4, but for the third-order dipole vector solitary wave with $q = 0.8$.

4. Stability of dipole vector solitary waves

The stability of the dipole vector modes was tested by direct simulations of Eq. (1). The simulations also confirmed the validity of analytical solutions (9), by comparing them to their numerical counterparts. Figure 6 shows the comparison between analytical and numerical solutions of Eq. (1), the latter obtained by means of the split-step beam-propagation method (see, e.g., Ref. [31], for a recent application of this method in a similar setting; the beam-propagation method based on the fast Fourier transform was introduced in Ref. [32]; in another context, the Fourier transform for the spatial dependence was introduced in Ref. [33] in combination with the leap-frog scheme for advancement in time). To this end, we solved Eq. (1) with initial conditions given by the exact solution (9) in $z = 0$ and larger values of q. It is seen that the analytical solution is consistent with the numerical results. Here, we keep the same parameters as in Fig. 3, but increase the modulation depth to $q = 0.95$, which allows us to obtain a remarkably stable state [we remind that setting $q = 1$ in Eq. (4) corresponds to the transition to the scalar solitary mode]. The general conclusion is that the stability of the dipole vector modes is strongly affected by q and improves for $q \rightarrow 1$.

The effective ("convective") stabilization of the expanding ring-shaped structure may be explained in a qualitative way. To this end, we notice that a straightforward analysis of the dimension of different terms in the underlying equation (1), with $f(I) = I$, predicts that the growth rate of the strongest instability of the vortex ring in a local Kerr medium against splitting by azimuthal perturbations [21] scales as $\gamma \sim \left(|A|^2\right)_{max}$ with the squared maximum amplitude of the nonlinear structure [22]. This estimate pertains to the quasi-stationary soliton (i.e., the one slowly expanding in a self-similar fashion), whose width scales as $\left(|A|\right)_{max}^{-1}$, which obviously complies with the conservation of the total power of the soliton. In a more accurate form, the above estimate is presented by the linear dependence of the growth rate of the stationary scalar vortex soliton on the soliton's propagation constant (κ), at small values of κ, as per Fig. 7 of Ref. [22] (a similar estimate was also given in Ref. [34]). Then, considering that the squared amplitude of the radially expanding ring decays with z according to Eq. (10), we conclude that the accumulated splitting perturbation grows as $\exp\left[const \cdot \int^z (z')^{-2} dz'\right]$. Because the integral in this expression converges for $z \rightarrow \infty$, the growth of the perturbation is bounded, and *does not* necessarily lead to the destruction of the structure. As for the instability against the collapse or decay, rather than the splitting, it is weaker than the splitting, as it grows with z not exponentially, but according to a power law [21].
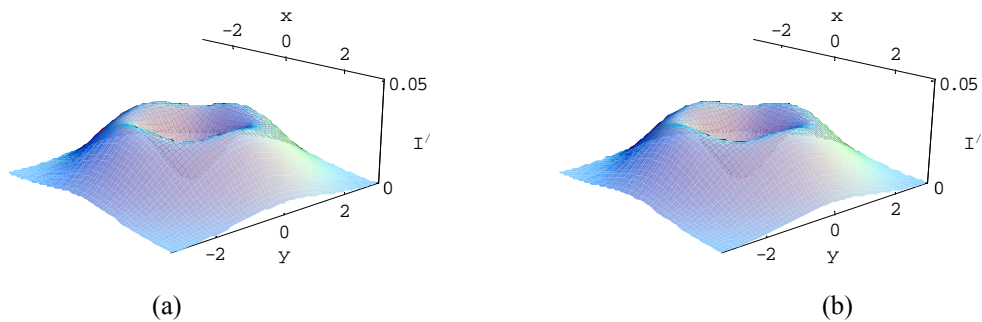

(a)   (b)

FIG. 6 (Color online) Comparison of the analytical solution (9), panel (a), with numerical simulations, at $z = 50$, panel (b). The parameters are as in Fig. 3, except for $q = 0.95$. As in Figs. 3-5, the intensity of the vector solitary wave is $I' = |u_1|^2 + |u_2|^2$. A tiny mismatch between the two plots is a result of the finite accuracy of the numerical simulations, which are quite sensitive to details of the numerical scheme, in this case.

5. Conclusions

We have generalized the class of self-trapped beam solutions of the nonlinear Schrödinger equation in the form of scalar vortices and vortical vector solitary waves, with necklace-type structure. We have demonstrated that such nonstationary (expanding) solitary modes may be effectively stable, proposing a qualitative explanation of the "convective" stabilization. The solutions of the coupled 2D Schrödinger equations with a self-focusing Kerr nonlinearity were obtained in both analytical and numerical forms (using the Hirota method for the former). The numerical analysis confirmed the existence of an extended family of dipole vector spatial solitary waves.

Appendix

Similar to Eq. (8), the second-order solitary-wave solutions to Eq. (5) can be obtained from Eq. (7) by setting $\varepsilon = 1$:

$$V^{(2)}(r,z) = r\frac{g_1(z,r) + g_3(z,r)}{1 + f_2(z,r) + f_4(z,r)}, \tag{A}$$

where we define

$$g_1 = \frac{e^{\theta_1}}{(C_1 + 2iz)^2} + \frac{e^{\theta_2}}{(C_2 + 2iz)^2}, \tag{B1}$$

$$f_2 = \frac{1}{4}\left[\frac{e^{\theta_1 + \theta_1^*}}{(C_1 + C_1^*)^2} + \frac{e^{\theta_1 + \theta_2^*}}{(C_1 + C_2^*)^2} + \frac{e^{\theta_2 + \theta_1^*}}{(C_2 + C_1^*)^2} + \frac{e^{\theta_2 + \theta_2^*}}{(C_2 + C_2^*)^2}\right], \tag{B2}$$

$$g_3 = \frac{(C_1^* - 2iz)^2 (C_1 - C_2)^2 e^{\theta_1 + \theta_2 + \theta_1^*}}{4(C_1 + 2iz)^2 (C_2 + 2iz)^2 (C_1 + C_1^*)^2 (C_2 + C_1^*)^2} + \frac{(C_2^* - 2iz)^2 (C_1 - C_2)^2 e^{\theta_1 + \theta_2 + \theta_2^*}}{4(C_1 + 2iz)^2 (C_2 + 2iz)^2 (C_2 + C_2^*)^2 (C_1 + C_2^*)^2}, \tag{B3}$$

$$f_4 = \frac{(C_1 - C_2)^2 (C_1^* - C_2^*)^2 e^{\theta_1 + \theta_1^* + \theta_2 + \theta_2^*}}{16(C_1 + C_1^*)^2 (C_2 + C_2^*)^2 (C_1 + C_2^*)^2 (C_2 + C_1^*)^2}, \tag{B4}$$

with $\theta_l = D_l - \dfrac{i}{8(C_l + C_l^*)\sqrt{C_l C_l^*}}\arctan\left(\dfrac{2z}{\sqrt{C_l C_l^*}}\right) - \dfrac{r^2}{C_l + 2iz}$ and both C_l and D_l being complex constants $(l = 1,2)$. More generally, we can obtain the Lth-order solitary-wave solutions of Eq. (5), as defined in Ref. [28], in the form of

$$V^{(L)}(r,z) = r\frac{g(r,z)}{f(r,z)}, \tag{C}$$

where

$$g(r,z) = \sum_{\mu=0,1}{}'\exp\left[\sum_{k=1}^{2N}\mu_k\chi_k + \sum_{k<j}^{2N}\Gamma(k,j)\mu_k\mu_j\right], \tag{D1}$$

8

$$g^*(r,z) = \sum_{\mu=0,1}{}'' \exp\left[\sum_{k=1}^{2N}\mu_k\chi_k + \sum_{k<j}^{2N}\Gamma(k,j)\mu_k\mu_j\right], \tag{D2}$$

$$f(r,z) = \sum_{\mu=0,1}{}''' \exp\left[\sum_{k=1}^{2N}\mu_k\chi_k + \sum_{k<j}^{2N}\Gamma(k,j)\mu_k\mu_j\right], \tag{D3}$$

with

$$\chi_k = a_k(z)r^2 + b_k(z) \quad,\quad a_k(z) = -\frac{1}{C_k+2iz} \quad,\quad b_k = D_k - \frac{i}{8(C_k+C_k^*)\sqrt{C_kC_k^*}}\arctan\left(\frac{2z}{\sqrt{C_kC_k^*}}\right) - 2\ln|a_k(z)| \quad \text{for}$$

$k=1,2,\cdots 2N$, and $\chi_{k+N}=\chi_k^*$, $a_{k+N}=a_k^*$, $b_{k+N}=b_k^*$; $\Gamma(k,j)=-2\ln|2a_k(z)+2a_j(z)|$, for $k=1,2,\cdots N$, and

$j=N+1,\cdots,2N$, or $k=N+1,\cdots,2N$, and $j=1,2,\cdots,N$;

$\Gamma(k,j)=2\ln|2a_k(z)-2a_j(z)|$, for $k=1,2,\cdots N$, and $j=1,2,\cdots,N$, or $k=N+1,\cdots,2N$, and $j=N+1,\cdots,2N$.

Here C_k and D_k are complex constants ($k=1,2,\cdots,2N$), $\sum_{k<j}^{2N}$ stands for the summation over all possible combinations of $2N$ elements taken with $k<j$, while $\sum_{\mu=0,1}{}'$, $\sum_{\mu=0,1}{}''$, $\sum_{\mu=0,1}{}'''$ denote the summation over all possible combinations of $\mu_k=0,1$ ($k=1,2,\cdots,2N$), satisfying the following relationships:

$$\sum_{k=1}^{N}{}'\mu_k = \sum_{k=1}^{N}{}'\mu_{k+N}, \qquad \sum_{k=1}^{N}{}''\mu_k = 1 + \sum_{k=1}^{N}{}''\mu_{k+N}, \qquad \sum_{k=1}^{N}{}'''\mu_{k+N} = 1 + \sum_{k=1}^{N}{}'''\mu_k.$$

References

[1] Y.S. Kivshar and B.A. Malomed, Rev. Mod. Phys. **61**, 765 (1989).

[2] M.S. Petrovic, M.R. Belic, C. Denz, and Y.S. Kivshar, Laser Photonics Rev. **5**, 214 (2011).

[3] Yu. S. Kivshar and G. Agrawal, *Optical solitons: from fibers to photonic crystals* (Academic, 2003).

[4] Z. Xu, Y. V. Kartashov, and L. Torner, Phys. Rev. E **73**, 055601 (2006).

[5] Y. V. Kartashov, L. Torner, V. A. Vysloukh, and D. Mihalache, Opt. Lett. **31**, 1483 (2006).

[6] A. Alberucci, M. Peccianti, G. Assanto, A. Dyadyusha, and M. Kaczmarek, Phys. Rev. Lett. **97**, 153903 (2006); G. Assanto, N. F. Smyth and A. L. Worthy, Phys. Rev. A **78**, 013832 (2008)

[7] Y. V. Izdebskaya, V. G. Shvedov, A. S. Desyatnikov, W. Z. Krolikowski, M. Belic, G. Assanto, and Y. S. Kivshar, Opt. Express **18**, 3258 (2010)

[8] G. Assanto and G. I. Stegeman, Opt. Express **10**, 388 (2002); G. Leo and G. Assanto, "Features and Applications of $\chi^{(2)}$ Vector Spatial Solitons", in "*Soliton Driven Photonics*", ed. by A. D. Boardman and A. P. Sukhorukov, pp. 77-86, (Kluwer Academic Publ., Dordrecht, 2001)

[9] W. E. Torruellas, Z. Wang, D. J. Hagan, E. W. van Stryland, G. I. Stegeman, L. Torner, and C. R. Menyuk, Phys. Rev. Lett. **74**, 5036 (1995); R. Schiek, Y. Baek, and G. I. Stegeman, Phys. Rev. E **53**, 1138 (1996); W. E. Torruellas, G. Assanto, B. L. Lawrence, R. A. Fuerst, and G. I. Stegeman, Appl. Phys. Lett. **68**, 1449 (1996); G. Leo, L. Colace, A. Amoroso, A. Di Falco, and G. Assanto, Opt. Lett. **28**, 1031 (2003); G. Leo, A. Amoroso, L. Colace, G. Assanto, R. V. Roussev, and M. M. Fejer, Opt. Lett. **29**, 1778 (2004).

[10] C. Etrich, F. Lederer, B. A. Malomed, T. Peschel, and U. Peschel, in: Progress in Optics (*ed.* by E. Wolf), vol. 41, p. 483 (Elsevier, Amsterdam, 2000); A. V. Buryak, P. Di Trapani, D. V. Skryabin, and S. Trillo, Phys. Rep. **370**, 63 (2002).

[11] X. Liu, L. J. Qian, and F. W. Wise, Phys. Rev. Lett. **82** 4631 (1999); B. A Malomed, D. Mihalache, F. Wise, and L.Torner, J. Opt. B: Quantum Semiclass. Opt. **7**, R53 (2005).

[12] J. J. Garcia-Ripoll, V. M. Perez-Garcia, E. A. Ostrovskaya, and Yu. S. Kivshar, Phys. Rev. Lett. **85**, 82 (2000).

[13] Z. Xu, N. F. Smyth, A. A. Minzoni, and Yu. S. Kivshar, Opt. Lett. **34**, 1414 (2009).

[14] W. Krolikowski, E.A. Ostrovskaya, C. Weilnau, *et al*., Phys. Rev. Lett. **85**, 1424 (2000).

[15] W. Krolikowski, G. McCarthy, Yu. S. Kivshar, *et al*., Phys. Rev. E **68**, 016612 (2003).

[16] V. M. Lashkin, E. A. Ostrovskaya, A. S. Desyatnikov, and Yu. S. Kivshar, Phys. Rev. A **80**, 013615 (2009).

[17] C. Rotschild, M. Segev, Z. Xu, Y.V. Kartashov, L. Torner, and O. Cohen, Opt. Lett. **31**, 3312 (2006).

[18] M. Shen, H. Ding, Q. Kong, L. Ruan, S. Pang, J. Shi, and Q. Wang, Phys. Rev. A **82**, 043815 (2010).

[19] F. Ye, B. A. Malomed, Y. He, and B. Hu, Phys. Rev. A **81**, 043816 (2010).

[20] M. Soljaćić and M. Segev, Phys. Rev. E **62**, 2810 (2000); A. S. Desyatnikov and Y. S. Kivshar, Phys. Rev. Lett. **87**, 033901 (2001); Y. V. Kartashov, G. Molina-Terriza, and L. Torner, J. Opt. Soc. Am. B **19**, 2682 (2002); D. Mihalache, D. Mazilu, L. C. Crasovan, B. A. Malomed, F. Lederer, and L. Torner, Phys. Rev. E **68**, 046612 (2003); Y. J. He, B. A. Malomed, H. Z. Wang, Opt. Exp. **15**, 17502 (2007); W. P. Zhong, M. Belić, R. H. Xie, and G. Chen, Phys. Rev. A **78**, 013826 (2008).

[21] B. A. Malomed, D. Mihalache, F. Wise, and L. Torner, J. Optics B: Quant. Semicl. Opt. **7**, R53 (2005).

[22] B. A. Malomed, L.-C. Crasovan, and D. Mihalache, Physica D **161**, 187 (2002).

[23] A.S. Desyatnikov and Y.S. Kivshar, Phys. Rev. Lett. **87**, 033901 (2001).

[24] W.P. Zhong and L.Yi, Phys. Rev. A **75**, 061801(R) (2007).

[25] W.P. Zhong and M. Belic, Phys. Rev. A79, 023804 (2009).

[26] R. Hirota, Phys. Rev. Lett. 27, 1192 (1971).

[27] W.P. Zhong and H. Luo, Chin. Phys. Lett. 8, 577 (2000).

[28] R. Hirota, J. Math. Phys. 14, 805 (1973).

[29] M. Soljacic, S. Sears, and M. Segev, Phys. Rev. Lett. **81**, 4851 (1998).

[30] M. Soljacic and M. Segev, Phys. Rev. E **62**, 2810 (2000).

[31] M. Belic, N. Petrovic, W.P. Zhong, R. H. Xie, and G. Chen, Phys. Rev. Lett.**101**, 123904 (2008).

[32] E. A. Sziklas and A. E. Siegman, Appl. Opt. **14**, 1874 (1975).

[33] B. Fornberg and G.B. Whitham, Phil. Trans. Roy. Soc. London A **289**, 373 (1978).

[34] A. A. Minzoni, N. F. Smyth, A. L, Worthy, and Y. S. Kivshar, Phys. Rev. A **76**, 063803 (2007).